

---

## Amplifying Nanosecond Optical Pulses at 1053 nm with an All-Fiber Regenerative Amplifier

Fiber optical amplifiers based on rare-earth-doped fibers have been investigated because of their advantages, including inherent compactness and stability, broadband gain, and good beam quality. The energy gain of conventional fiber amplifiers for low-duty-cycle pulse sources is limited by their single-pass design since broadband amplified spontaneous emission (ASE) competes for the gain and degrades the signal-to-noise ratio (SNR). This limitation can be overcome by implementing regenerative amplification in an all-fiber system. With a gain fiber in a fiber cavity, optical pulses circulate inside the cavity and gain energy in many round-trips. All-fiber regenerative amplifiers (AFRA's) greatly improve the energy gain and SNR, while preserving the advantages of an all-fiber architecture. A ring-cavity,  $Q$ -switched fiber regenerative amplifier based on Er-doped fiber demonstrated a gain of more than 40 dB for 10-ns, 3-pJ pulses at 1530 nm (Ref. 1). Another Yb-doped fiber regenerative amplifier operating at 1030 nm amplified 40-ps, 9-pJ pulses to 55 nJ (Ref. 2).

An important potential AFRA application is to produce chirped optical pulses to seed chirped-pulse-amplification (CPA) systems. An approximately quadratic temporal-phase profile (a linear frequency chirp) is required for CPA seed pulses to be amplified and then compressed by grating-pulse compressors.<sup>3</sup> The conventional approach to producing such seed pulses uses a mode-locked laser and a grating-pulse stretcher. This combination can be replaced by an AFRA with an electro-optic phase modulator (EOM) integrated inside the ring cavity.<sup>4</sup> The required temporal phase can be imposed onto the optical pulse during many round-trips inside the cavity. Compared with the conventional approach, such an all-fiber CPA seed source can provide precise and flexible control over the phase profile, higher seed pulse energy to increase the SNR and temporal contrast of the CPA output, single-mode and alignment-free operation, and increased cost effectiveness.

This article reports on an AFRA based on Yb-doped fiber to amplify nanosecond, 1053-nm optical pulses with a repetition rate of 10.5 kHz. The pulses are amplified from 15 pJ to 240 nJ in five passes through the gain fiber. To the best of our

knowledge, this is the highest AFRA output-pulse energy ever reported. The wavelength of the AFRA is required by existing high-energy CPA systems based on Nd-phosphate laser glass.<sup>5</sup> This wavelength is 23 nm off the gain peak of a Yb-doped fiber at 1030 nm, so ASE suppression techniques to favor the signal gain have been employed.<sup>6</sup> Cavity build-up dynamics evident from leakage-pulse measurements and numerical modeling shows that the AFRA is not saturated in five round-trips and higher pulse energy can be extracted in more round-trips.<sup>7</sup> This is limited, however, by the onset of bifurcation instability previously identified for solid-state regenerative amplifiers operating at high repetition rates.<sup>8</sup> This limitation can be lifted by reducing the repetition rate from 10.5 kHz to below 0.5 kHz. Numerical simulations show that operating the AFRA at saturation not only increases the output level but also improves the output stability.

The experimental AFRA setup is shown in Fig. 126.31. The amplifier is seeded by 10-ns square pulses at 1053 nm. A fiber ring cavity is built with a section of polarization-maintaining (PM) Yb-doped fiber (3.5-m, 6- $\mu$ m core, 30 $\pm$ 10 dB/m absorption at 980 nm) as the gain medium. The gain fiber is counter-pumped by a 500-mW continuous-wave diode laser at 976 nm (JDSU 29-7552-500) through a 976/1053-nm wavelength division multiplexer (WDM1). An additional 976/1053-nm WDM (WDM2) protects the pump diode against amplified optical signals at 1053 nm from the cavity. It provides 20-dB isolation over 1053 nm at the 976-nm port. A 2  $\times$  2 acousto-optic modulator (AOM) switch is used to switch the pulse in and out of the ring and to  $Q$ -switch the cavity. The two transmission states of the AOM switch, shown in the inset of Fig. 126.31, alternate the cavity between low- $Q$  and high- $Q$  phases. In the low- $Q$  phase, lasing is suppressed and the gain fiber accumulates stored energy from pumping. The fiber cavity is essentially a single-pass system in this state. The cavity is switched to the high- $Q$  phase after a seed pulse is injected, which gains energy in multiple passes through the gain fiber before being switched out at the end of this phase. A delay generator synchronized to the seed pulses controls the duration of the "on" state of the AOM and therefore the number of round-trips in the cavity. To

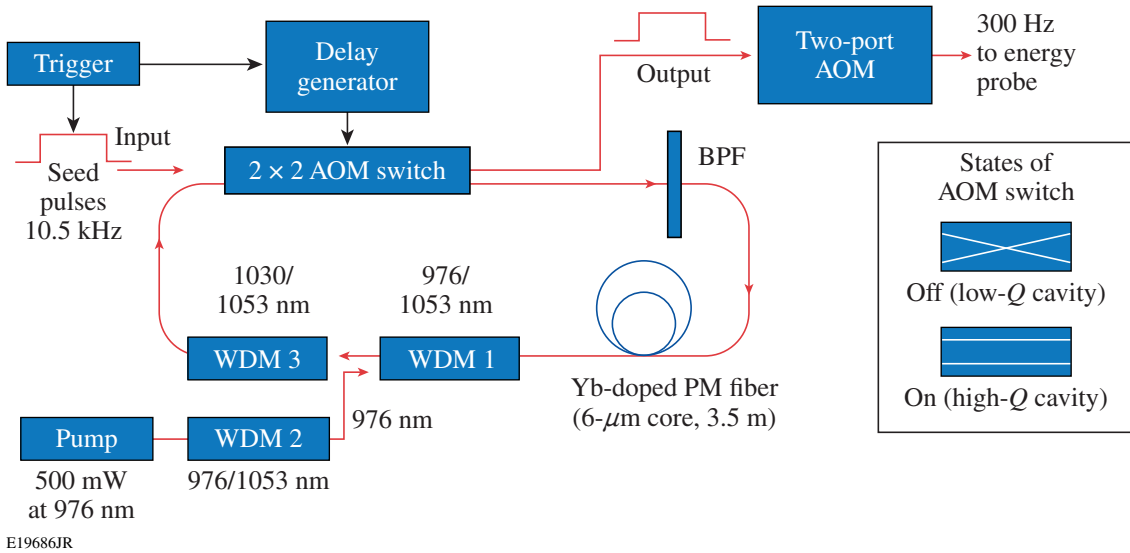
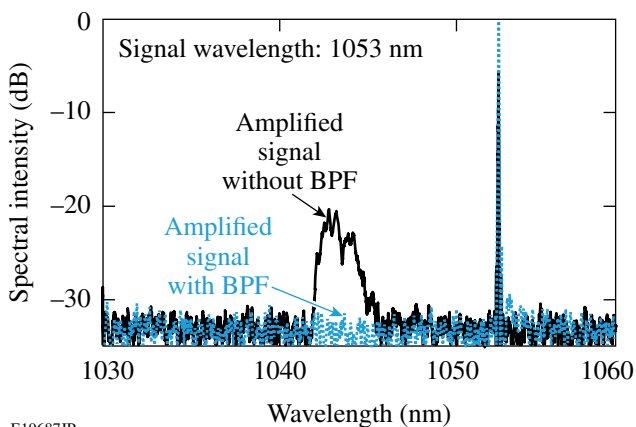


Figure 126.31

Experimental setup for the all-fiber regenerative amplifier (AFRA). In addition to the Yb-doped fiber as the gain medium, a 10-nm bandpass filter and a 1030/1053-nm WDM are built into the fiber cavity to suppress ASE and favor the signal gain. Optical pulses are switched in and out of the cavity by a  $2 \times 2$  AOM switch. The two states of the switch are shown on the right.

favor the signal gain, a 1030/1053-nm WDM (WDM3) suppresses the 1030-nm gain peak, and a 10-nm bandpass filter (BPF) centered at 1055 nm further suppresses ASE at 1042 to 1046 nm. The output-pulse train's repetition rate is reduced to 300 Hz by a two-port AOM to enable one to directly measure the output-pulse energy with an energy probe limited to a maximum 2-kHz rate.

The effects of the ASE suppression techniques are shown in Fig. 126.32. The solid curve shows the spectrum of a 10-nJ



E19687JR

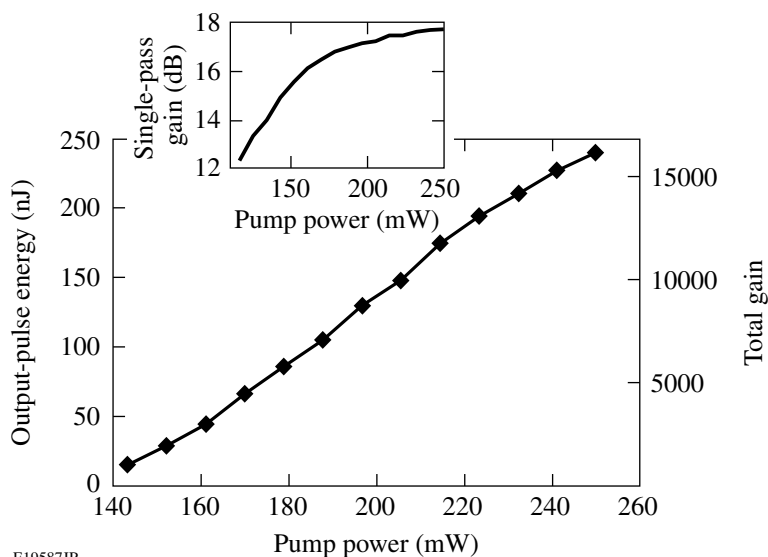
Figure 126.32

Spectra of 10-nJ output-pulse train from the fiber ring cavity without a BPF (dotted) and with a BPF (solid). The 1030-nm gain peak is suppressed by WDM3, and ASE at 1042 to 1046 nm is suppressed by the BPF.

output-pulse train without the bandpass filter in the cavity. WDM3 effectively suppresses ASE around 1030 nm, but ASE at 1042 to 1046 nm still develops. As the dotted curve shows, this ASE is completely suppressed by the bandpass filter. The bandpass filter also blocks any leakage pump beam from going back into the seed laser.

The 15-pJ seed pulses are amplified to 240 nJ in five round-trips in the cavity. Figure 126.33 shows the output-pulse energy and the total gain from five round-trips as the pump power is increased from 145 mW to 250 mW. The single-pass, small-signal gain of the Yb-doped fiber at pump levels up to 250 mW is plotted in the inset. Increasing the pump power beyond 250 mW does not increase the gain as the population inversion reaches maximum and additional pump is not absorbed, limiting the single-pass gain to about 18 dB and the total gain in five round-trips to 42 dB. At the highest output level, the pulse energy has a short-term (200 samples) fluctuation of 1.5% (rms) and a long-term drift of 6% (peak to valley).

Input and output pulses are measured using a 12-GHz photodiode (Discovery DSC50S) and single-shot oscilloscope (Tektronix DPO70604) to investigate the effect of the regenerative amplifier on the pulse shape. Normalized input and output waveforms are plotted in Fig. 126.34. The data are smoothed numerically to reduce instrumental noise. Compared to the input square pulse (solid), the output pulse (dashed) has a trailing edge 15% lower than the leading edge. This square-pulse



E19587JR

Figure 126.33

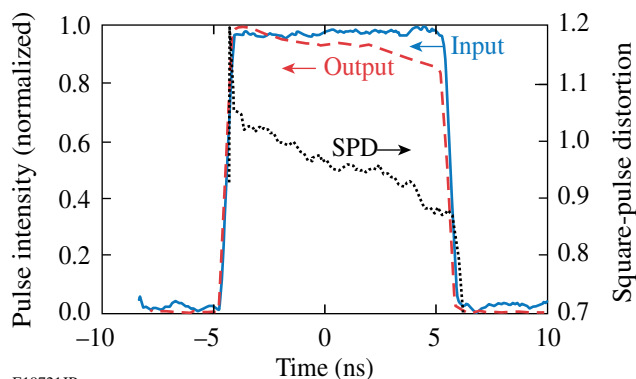
Measured pulse energy and total gain as pump power is increased. The pulse circulates in the ring cavity for five round-trips. Inset is the single-pass gain.

distortion (SPD), the ratio between the instantaneous intensities of the output pulse over the input pulse, originates from gain saturation of the regenerative amplifier and is also plotted (dotted) in Fig. 126.34.

Ideally for a regenerative amplifier, the pulse would circulate inside the cavity to accumulate energy until the stored energy is depleted and the gain is overcome by cavity loss (saturation). Maximum output-pulse energy is obtained when the pulse is ejected from the cavity at saturation. At the highest stable output level of the AFRA, the pulse energy increases exponentially (9 dB/RT) before cavity dump, which indicates that the amplifier does not saturate in five round-trips. This is further proved by numerical modeling.<sup>7</sup> The laser pulse

amplification and population inversion in the gain medium are governed by rate equations that can be integrated to yield recurrence relations. The pulse fluence (proportional to pulse energy) and single-pass gain in the regenerative amplifier can be calculated for each pass using these recurrence relations. The solid curve in Fig. 126.35(a) shows the growth in pulse energy and the dashed curve shows the gain for each pass, calculated with this model. The gain is hardly depleted in five round-trips, and the AFRA has the potential to produce much higher pulse energy in more round-trips.

Producing higher pulse energy in the AFRA by increasing the number of round-trips is limited by the onset of period-doubling instability, where the output-pulse energy switches between different values.<sup>8</sup> When the stored energy in the gain medium fully recovers through pumping between successive seed pulses, each pulse experiences the same gain and the output-pulse energy is stable. This may not be the case when the repetition rate of the regenerative amplifier is high enough that the time separation between seed pulses (cycle period) is comparable with or shorter than the upper-state lifetime of the gain medium. As the number of round-trips is increased and more energy is extracted in the high- $Q$  phase, the population inversion will not have an opportunity to fully recover in the following low- $Q$  phase because of its short duration. This reduces the gain for the next pulse and results in a lower pulse energy, which, in turn, leaves a larger amount of stored energy in the gain fiber to produce higher output in the cycle after the next. With the AFRA operating at 10.5 kHz, the cycle period ( $\sim 95 \mu\text{s}$ ) is much shorter than the Yb upper-state lifetime ( $\sim 840 \mu\text{s}$ ) and period-doubling instability is observed.



E19721JR

Figure 126.34

Input-pulse (solid) and output-pulse (dashed) shape and SPD (dotted) of the fiber amplifier. The output pulse has a 15%-lower trailing edge because of gain saturation.

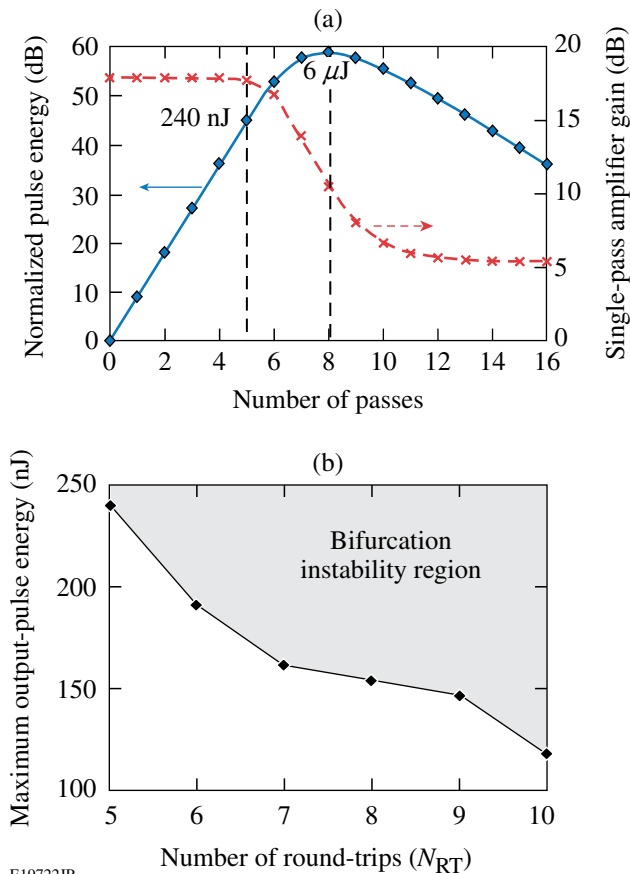


Figure 126.35

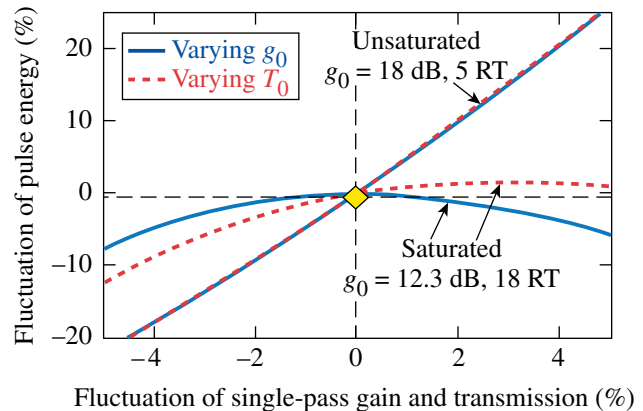
(a) Numerical simulation shows that the AFRA is not saturated after five round-trips and much higher pulse energy can be extracted from the amplifier in more round-trips. (b) The maximum stable output-pulse energy decreases when the number of round-trips is increased.

To avoid this, the pump level to the AFRA must be decreased as the number of round-trips increases. The maximum stable output-pulse energy decreases with more round-trips as shown in Fig. 126.35(b).

At repetition rates lower than 0.5 kHz, the cycle period will be long enough for the stored energy to fully recover.<sup>8</sup> The pulse would circulate in the cavity for more round-trips and gain higher energy without causing period-doubling instability. Scaling the AFRA to higher pulse energies requires investigating detrimental nonlinear effects such as stimulated Brillouin scattering (SBS) and stimulated Raman scattering (SRS). For a 10-ns pulse, the estimated threshold pulse energy is 1.5  $\mu$ J for SBS<sup>9</sup> and 5  $\mu$ J for SRS.<sup>10</sup> With the single-pass gain reduced to

12.3 dB, the numerical model described above shows that the amplifier can produce 1.5- $\mu$ J pulse energy in 17 round-trips at saturation.

Operating the AFRA at saturation will not only increase the output level but also improve the output stability. As mentioned above, the AFRA output-pulse energy fluctuates because of variations in amplifier parameters like the single-pass small-signal gain ( $g_0$ ) and loop transmission ( $T_0$ ). The sensitivity of the output-pulse energy with respect to these parameters is determined by varying them in the numerical model described above. Figure 126.36 compares the output sensitivities of two operating points: five round-trips with a single-pass gain of 18 dB (unsaturated) and 18 round-trips with a single-pass gain of 12.3 dB (saturated). For the unsaturated case, the output fluctuation is 5 $\times$  any variation of  $g_0$  and  $T_0$ . The output sensitivity is greatly reduced for the saturated case. Operating the amplifier for one round-trip after maximum pulse energy (reached in 17 round-trips) yields the best stability, with only 2% of energy penalty.



E19723JR

Figure 126.36

Variation of the amplifier output-pulse energy as small-signal gain (solid) and loop transmission (dashed) are varied. Comparing the output sensitivities of the saturated and unsaturated AFRA, it is found that operating the amplifier at saturation will greatly improve the output stability.

In conclusion, an all-fiber regenerative amplifier with Yb-doped fiber as the gain medium has been built. Nanosecond optical pulses at 1053 nm (23 nm off the gain peak of Yb-doped fiber) were amplified to as much as 240 nJ by the amplifier, achieving a total gain of 42 dB. The AFRA output level is limited by the onset of bifurcation instability previously iden-

tified for solid-state regenerative amplifiers operating at high repetition rates. Higher pulse energy may be expected from the AFRA at repetition rates lower than 0.5 kHz, limited by SBS. Sensitivity of the output-pulse energy with respect to amplifier parameters has been tested with numerical simulation, which suggests that operating the amplifier at saturation will greatly improve the output stability. The hundreds-of-nJ output-pulse energy makes the AFRA an attractive candidate as a CPA seed source (once a phase modulator is integrated into the cavity), compared to hundreds-of-pJ seed pulses commonly used in existing high-energy CPA systems.<sup>5</sup>

#### ACKNOWLEDGMENT

The authors are grateful for numerous conversations with and helpful support from J. R. Marciante, A. V. Okishev, and W. Bittle.

This work was supported by the U.S. Department of Energy Office of Inertial Confinement Fusion under Cooperative Agreement No. DE-FC52-08NA28302, the University of Rochester, and the New York State Energy Research and Development Authority. The support of DOE does not constitute an endorsement by DOE of the views expressed in this article.

#### REFERENCES

1. A. Yang, *Jpn. J. Appl. Phys.* **45**, L673 (2006).
2. S. Kanzelmeyer *et al.*, presented at Advanced Solid-State Photonics (ASSP), San Diego, CA, 31 January–3 February 2010 (Paper AWB15).
3. D. Strickland and G. Mourou, *Opt. Commun.* **56**, 219 (1985).
4. R. Xin and J. D. Zuegel, presented at Advanced Solid-State Photonics (ASSP), San Diego, CA, 31 January–3 February 2010 (Paper AMD3).
5. J. D. Zuegel, S. Borneis, C. Barty, B. LeGarrec, C. Danson, N. Miyanaga, P. K. Rambo, C. LeBlanc, T. J. Kessler, A. W. Schmid, L. J. Waxer, J. H. Kelly, B. Kruschwitz, R. Jungquist, E. Moses, J. Britten, I. Jovanovic, J. Dawson, and N. Blanchot, *Fusion Sci. Technol.* **49**, 453 (2006).
6. J. R. Marciante and J. D. Zuegel, *Appl. Opt.* **45**, 6798 (2006).
7. W. H. Lowdermilk and J. E. Murray, *J. Appl. Phys.* **51**, 2436 (1980).
8. J. Döring *et al.*, *Opt. Express* **12**, 1759 (2004).
9. H. Li and K. Ogusu, *Jpn. J. Appl. Phys.* **38**, 6309 (1999).
10. R. G. Smith, *Appl. Opt.* **11**, 2489 (1972).